

A MEASUREMENT OF THE NEUTRON
DIFFUSION PARAMETERS OF WATER AT DIFFERENT
TEMPERATURES BY THE PULSED METHOD*

by

John Arthur McClure

Dissertation submitted to the Graduate Faculty of
the Virginia Polytechnic Institute
in candidacy for the degree of
DOCTOR OF PHILOSOPHY
in
Physics

October 1962

Blacksburg, Virginia

*Supported in part by the United States Atomic Energy Commission

TABLE OF CONTENTS

	Page
I. INTRODUCTION.....	5
II. EXPERIMENTAL APPARATUS AND PROCEDURE.....	6
A. Accelerator.....	6
B. Time Analyser.....	10
C. Measurement Technique.....	17
D. Data Analysis.....	21
E. Calculation of B^2	23
III. REVIEW OF LITERATURE.....	27
IV. RESULTS AND DISCUSSION.....	36
A. Results of Measurements.....	36
B. Sources of Error.....	42
V. ACKNOWLEDGEMENTS.....	43
VI. BIBLIOGRAPHY.....	44
VII. VITA.....	48
VIII. APPENDIX - THEORY OF PULSED NEUTRON MEASUREMENTS.....	49

LIST OF FIGURES

	Page
Fig. 1 Instrumentation for Pulsed Experiments.....	8
Fig. 2 10 μ sec to 20 μ sec Channel Width Converter.....	11
Fig. 3 150 v Regulated Power Supply.....	12
Fig. 4 Pulse Amplifier For Scalers.....	13
Fig. 5 Experimental Arrangement.....	18
Fig. 6 Temperature Dependence of Diffusion Coefficient D_0	33
Fig. 7 Temperature Dependence of Diffusion Cooling Coefficient C.....	34
Fig. 8 Decay Constants as a Function of B^2 For Water at 1.0°C.....	38
Fig. 9 Decay Constants as a Function of B^2 For Ice at -19°C.....	39

LIST OF TABLES

		Page
Table I	Neutron Diffusion Parameters in Water at 22°C.....	28
Table II	Neutron Diffusion Parameters in Water Kuchle ⁽⁷⁾ ...	28
Table III	Neutron Diffusion Parameters in Water Antonov ⁽¹²⁾ ..	30
Table IV	Decay Constants Measured at 1.0°C.....	37
Table V	Decay Constants Measured at -19°C.....	37
Table VI	Diffusion Coefficients of Water From This Experiment.....	41

I. INTRODUCTION

The interaction of neutrons with matter investigated by the pulsed neutron source method has received considerable attention in recent years both theoretically and experimentally. The pulsed source method is well suited for measuring the diffusion parameters of neutron moderator materials. A moderator material is characterized by a low atomic weight for efficient neutron thermalization and by a low neutron absorption cross section to optimize neutron economy. The neutron diffusion parameters in moderators are functions of the velocity of the neutrons.

Data for moderators at high temperatures are particularly valuable to the designers of power reactors. However, to properly understand the physical processes involved in neutron thermalization, the diffusion parameters need to be measured from very low to quite high temperatures. This thesis reports an investigation of the diffusion parameters of light water by the pulsed source method in the temperature range -20°C to 25°C . Most of the work done on water to date has been above 20°C , and no results have been reported on any experiments by the pulsed method in ice just below the freezing point.

II. EXPERIMENTAL APPARATUS AND PROCEDURE

A. Accelerator

A portable Cockcroft-Walton accelerator was constructed by the author to serve as a pulsed neutron source. The ion source, described by Morris⁽¹³⁾, is operated at a positive potential with respect to the target which is at ground potential.

The accelerating voltage is supplied from a transformer rectifier power supply manufactured by Beta Electronics, Inc. Although the manufacturer rates the power supply at 0-250,000 volts dc of either positive or negative polarity, difficulty has been experienced in obtaining reliable operation at the maximum voltage. The experiments were carried out at around 150,000 volts.

A pressure of the order of 10^{-5} millimeters of mercury is maintained within the accelerator by an oil diffusion pump (Type MCF-300 manufactured by Consolidated Vacuum Corporation). When the pressure in the accelerator, measured by a VG-1A ionization gauge, rises above a present level, a safety relay is activated which turns off both the VG-1A filament and the diffusion pump heater. The VG-1A filament and diffusion pump heater remain off until manually reset.

Neutrons in the 2-3 Mev. range can be produced by the accelerator from the ${}^2_1\text{H}(d, n){}^3_2\text{He}$ reaction. A greater yield of neutrons can be obtained by using the reaction ${}^3_1\text{H}(d, n){}^4_2\text{He}$. The yield for this reaction is $\sim 10^8$ n/microcoulomb for $E_d = 200$ kilovolts⁽²²⁾; where

E_d is the accelerator potential. Neutrons from the D-T reaction are practically monenergetic at 14.7 Mev. The tritium reaction was selected because of the greater neutron yields and correspondingly improved counting rates.

The tritium targets used in the experiment were obtained from the Isotope Division of Oak Ridge National Laboratories. The targets are fabricated by vapor plating 500 micrograms per square centimeter of pure zirconium metal on one surface of a 0.25 millimeter thick platinum disk. The zirconium is then impregnated with tritium. The guaranteed minimum ${}^1\text{H}^3\text{-Zr}$ atomic ratio is 1:1, or slightly over 310 millicuries of tritium per milligram of zirconium; however, each target is impregnated with the maximum amount of tritium⁽¹¹⁾. Diameter of the target used was 3.2 centimeters.

Neutron pulses are produced by modulating the deuteron beam in the accelerator. A simple pulsing system was used in the experiment although a somewhat more elaborate system has been developed⁽³¹⁾. A positive potential applied to deflection plates placed in the accelerator tube at the ground potential end moves the beam to one side of the central axis. A system of baffles prevents the beam from reaching the target unless it travels on the central axis. A reference pulse from a time analyser (Fig. 1), to be described later, triggers a Hewlett-Packard 212-A pulse generator which produces a positive square pulse whose width is variable from 0.1 to 10 microseconds. A pulse width of 10 microseconds was chosen to provide satisfactory neutron

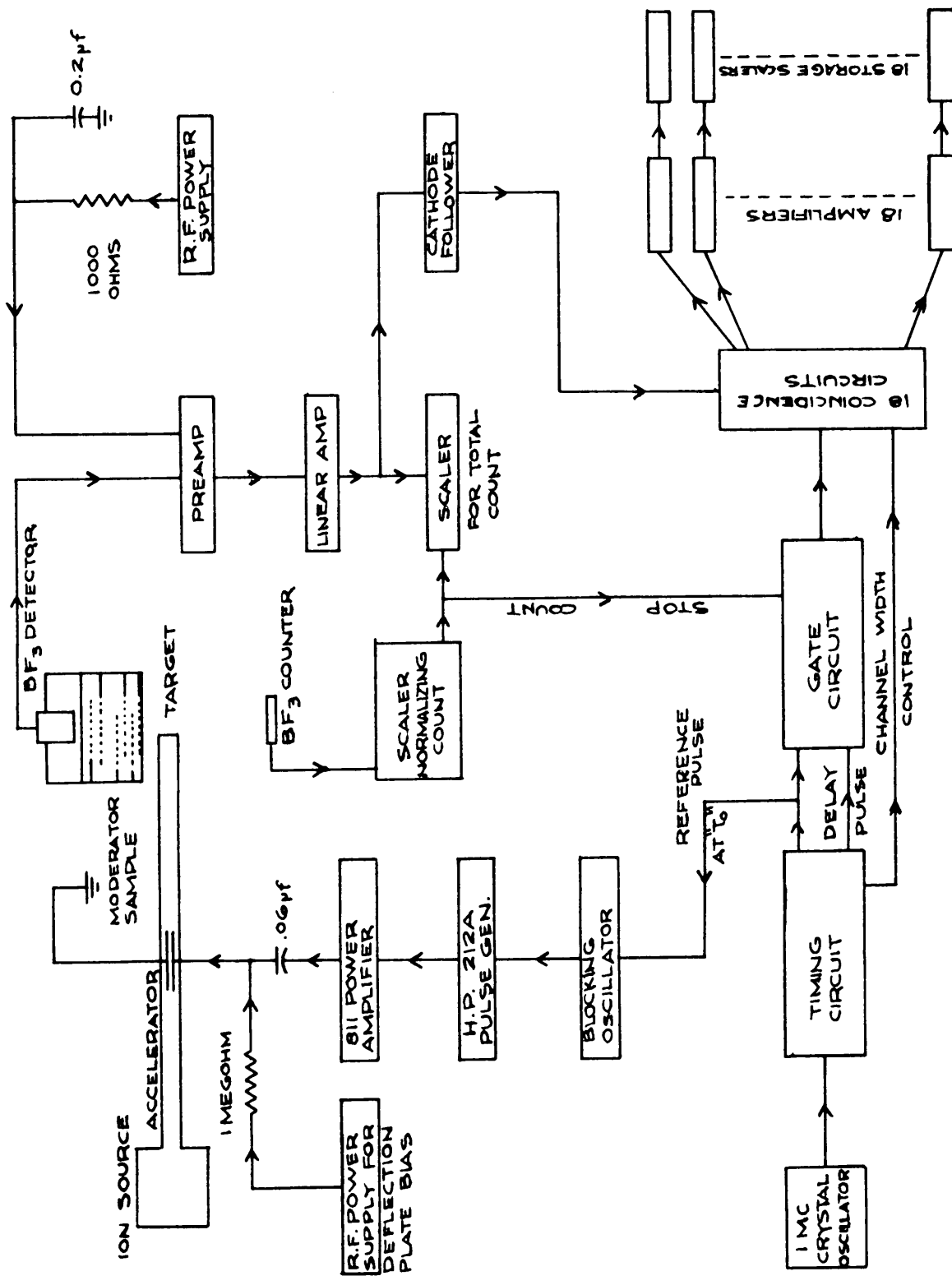


FIG. 1. INSTRUMENTATION FOR PULSED EXPERIMENTS

production per pulse. The square wave is amplified by an 811 power triode and applied to the deflection plates through a blocking capacitor. The bias voltage on the deflection plates is adjusted until the pulsed beam current on the target is a maximum. Provision is made to monitor the total beam current where it strikes a baffle. A current meter and charge integrator designed by Higgenbotham⁽¹⁶⁾ was constructed to measure the charge collected by the target. Currents in the order of 100 microamperes have been obtained from the accelerator using a Moak type R. F. ion source. Currents between 20 and 40 microamperes steady state were used during the pulsed operation.

B. Time Analyser

To examine the time distribution of neutrons leaving a moderator following the injection of a burst of fast neutrons, an eighteen channel time analyser was constructed by the author. A complete schematic diagram of the time analyser appears in the pocket on the inside back cover. Figs. 2-4 are schematics of associated electronic circuits. The time analyser consists of a timing circuit which generates a standard time signal and a gate circuit which sorts the neutron pulses into their respective time channels.

Pulses from a master one-megacycle crystal oscillator are counted on Burroughs beam-switching tubes. A discussion of the operating characteristics of beam-switching tubes is given by Hollandsworth⁽¹⁴⁾. The tube has ten positions around which the electron beam advances cyclicly; consequently, the frequency division through the tube is ten. A signal may be obtained from any or all of the ten positions which the beam assumes in making a complete traverse around the tube. The timing circuit described has a possible frequency reduction of 10^5 .

The time measurements utilized as a reference pulse the leading edge of a pulse from the zeroth position of a given beam-switching tube. This pulse is coincident with a pulse on the zeroth position of each preceding beam switching tube. Suppose the electron beam is in the ninth position in each tube. Counting one more pulse will move the beam in each of the tubes to the zero position producing the reference pulse at the given tube. Possible choices available from the timing unit for the

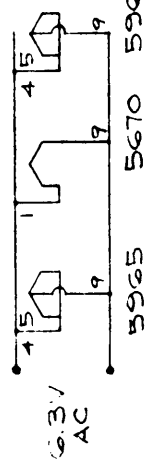
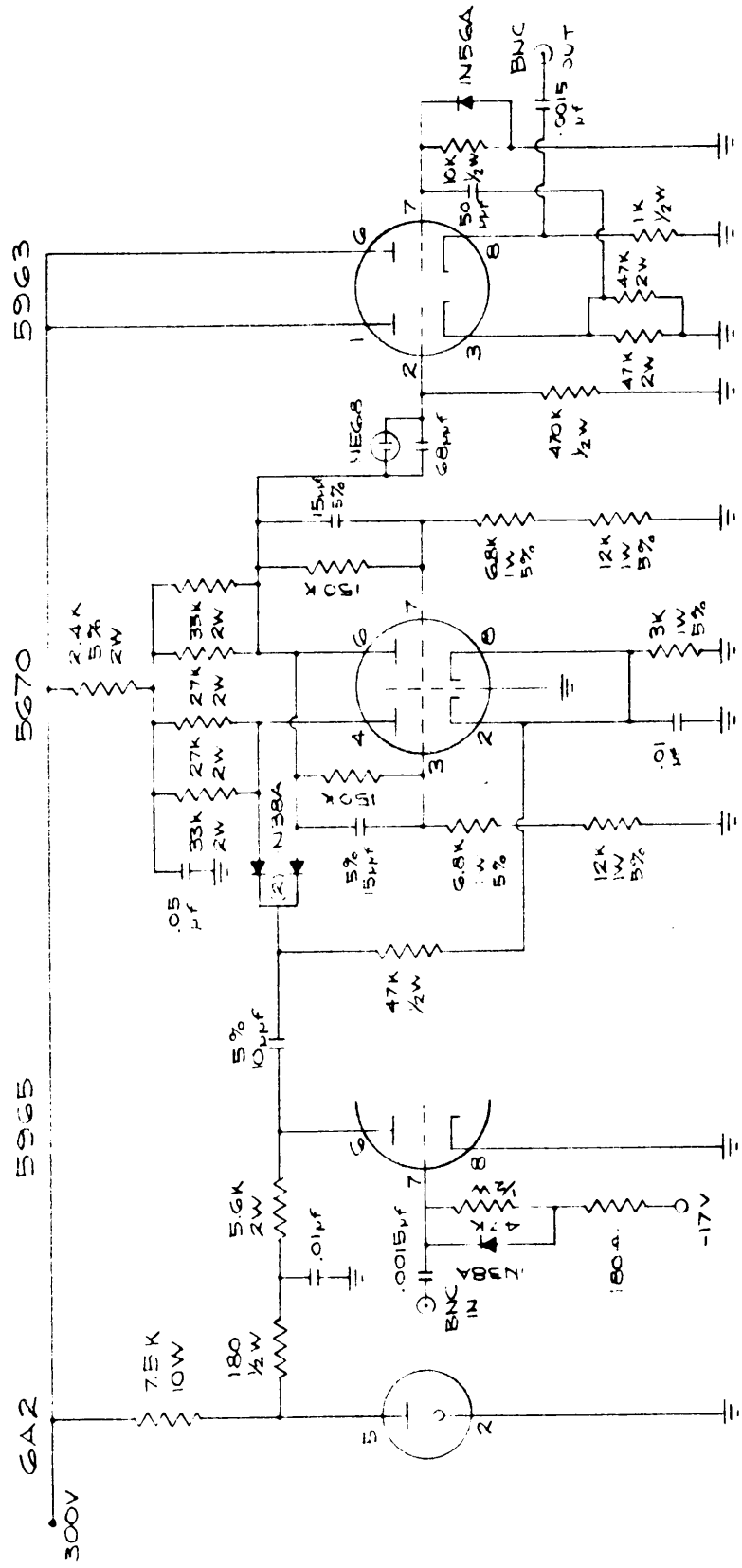


FIG. 2. 10 μsec to 20 μsec CHANNEL WIDTH CONVERTER

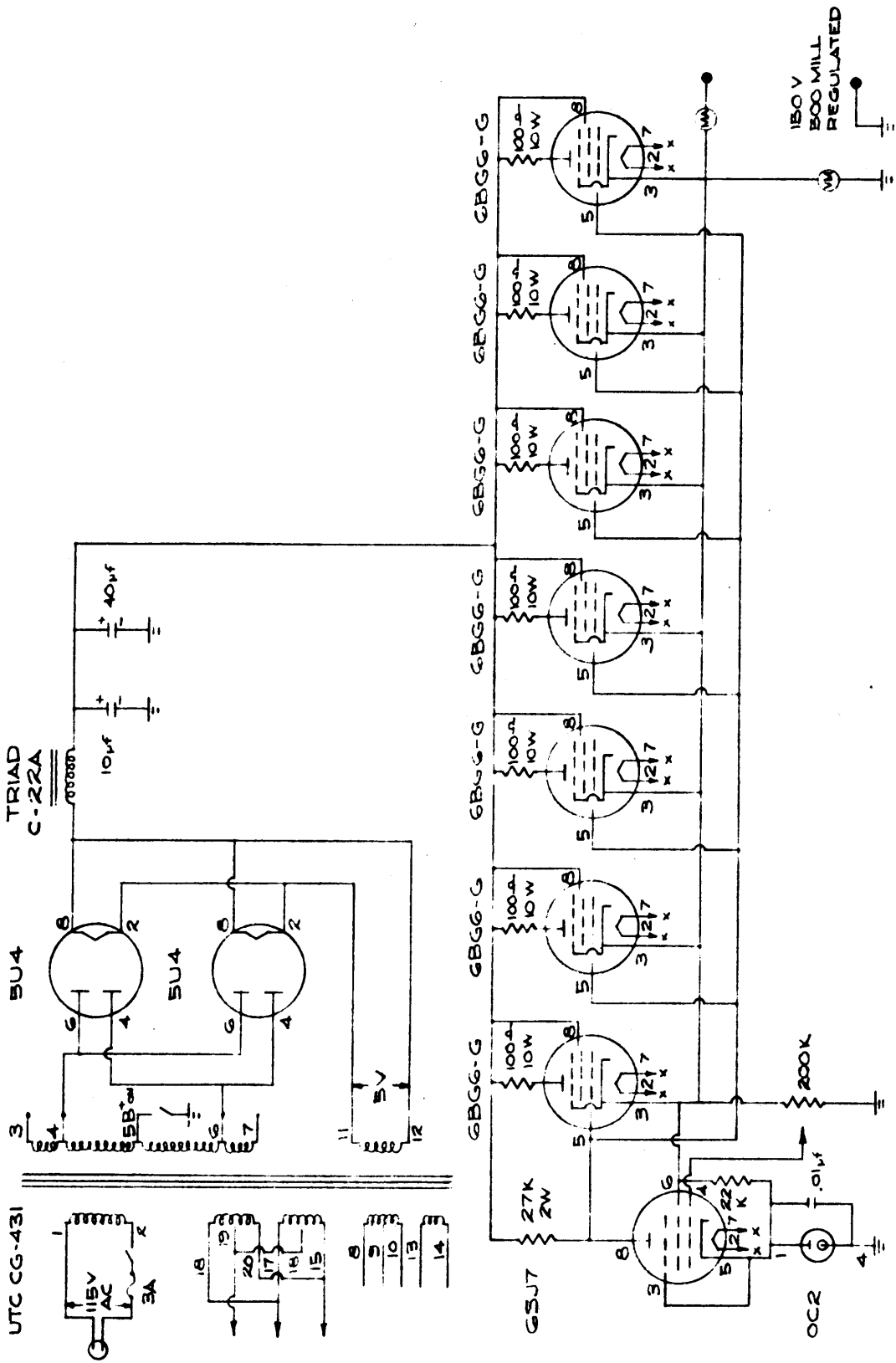


FIG 3. 150 V REGULATED POWER SUPPLY

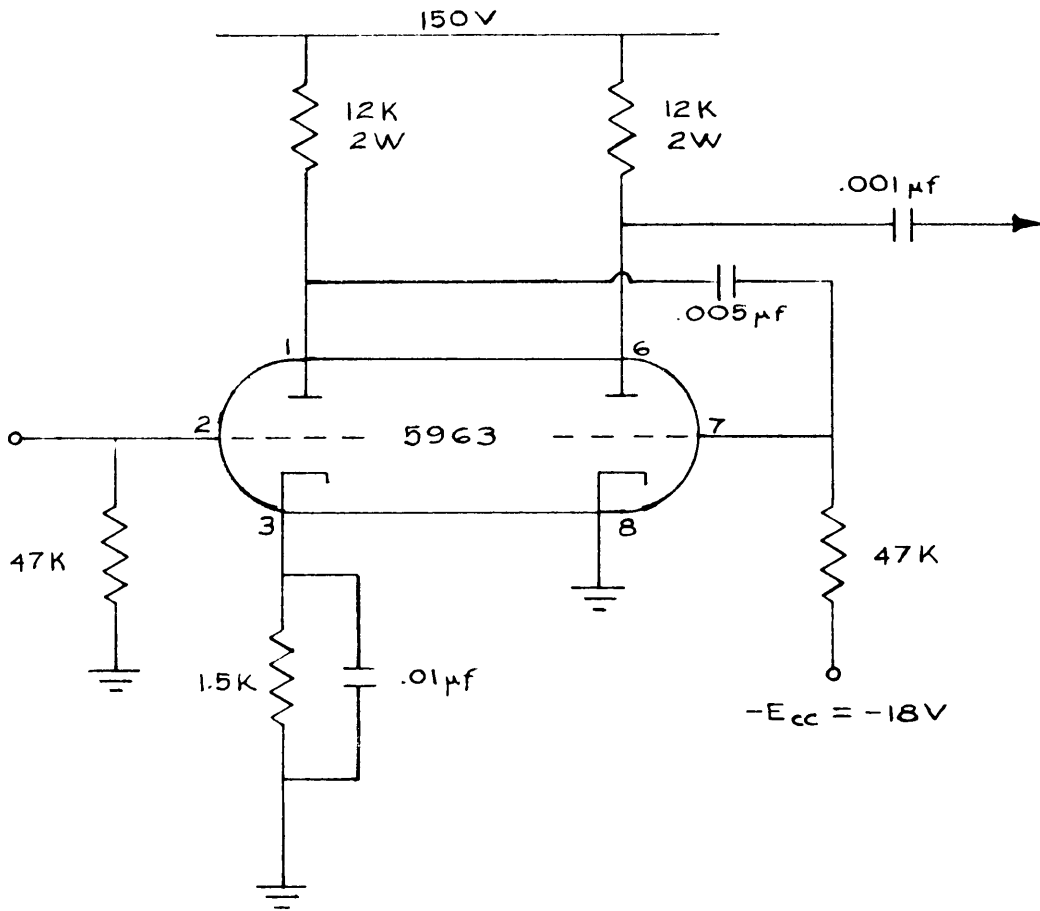


FIG. 4 PULSE AMPLIFIER FOR SCALERS

repetition rate of the reference time pulse are 10, 100, 1000, and 10,000 cycles per second. As previously mentioned, the reference pulse triggers a Hewlett-Packard 212-A pulse generator at the Cockcroft-Walton accelerator to produce a neutron burst. In addition, the reference pulse activates a delay multivibrator in the gate circuit which controls the start of the time channels.

Following the reference pulse, which occurs at, say, time t_0 , a pulse is available at a known later time, t_1 , by differentiating the leading edge of the wave from the target* of the proper beam-switching tube. The delay time, t_1 , is not continuously variable but must be chosen from one of the following set: 1, 2, 3,, 9 microseconds; 10, 20, 30,, 90 microseconds; 100, 200, 300,, 900 microseconds; 1, 2, 3,, 9 milliseconds; 10, 20, 30,, 90 milliseconds. Only one range may be used at a time, with the preselected delay time obtained via a switch; the remaining switches being in the "off" position. Furthermore, the choice in delay time is subject to two restrictions: the total time to sequence through the the eighteen channels plus the delay time must not exceed the time between reference pulses, and secondly, the delay time must be equal to or greater than the channel width.

The delay pulse is sent to the second side of the same binary in the gate circuit as is the reference pulse, causing the binary to change states. A negative signal is obtained which pulses the zero grid of a Burroughs BD-316 beam switching tube. The BD-316 tube incorporates a separate switching grid in the zero position which enables

* One of the anodes in a beam-switching tube

the grid to be used as a gate. Whenever the beam is in that position, pulsing the odd and even grids will not cause the beam to advance.

The binary which drives the odd and even switching grids of the BD-316 tubes is reset by the delay pulse to the proper phase such that the first grid pulsed after t_1 will always be the odd grid. As the binary runs continuously at a higher frequency than the delay pulse, resetting the binary by the delay pulse limits the choice of delay times to a whole multiple of the channel width.

Targets one through nine of the BD-316 tubes in the gate circuit are directly coupled to one side of coincidence circuits forming the respective channels. Eighteen channels are obtained by using two BD-316 tubes in series. The delay pulse at t_1 triggers the zero grid of the first BD-316, advancing the beam to position one and opening channel one. The beam is then advanced around the BD-316, opening channels two through nine in succession. Upon returning to the zero position, operation is shifted to the second BD-316 which opens channels ten through eighteen.

Neutron pulses from the BF_3 detector are applied simultaneously to the second side of all the coincidence circuits. Counts are recorded in a channel only during the time the beam in the BD-316 is on the respective target. Neutron counts from each channel are stored in scalars.

The channel width is controlled by the frequency of the binary which drives the odd and even switching grids. Four possible channel

widths are available, viz.; 1 microsecond, 10 microseconds, 100 microseconds, and 1000 microseconds. Channel width measurements were made in the following manner. A BF_3 detector counted a random source of neutrons. The pulses were fed into the total count scaler and also the time analyser. The channel width is proportional to the ratio of the number of counts in the channel to the total count.

C. Measurement Technique

The pulsed measurements were carried out in a large paraffin shield (Fig. 5) which served the double role of a thermal insulator for the refrigerator and an absorber of scattered neutrons. Scattered neutrons were prevented from entering the samples by covering the containers with 30 mils of cadmium. The cooling coils for the refrigerator were wound in a helix at the outside edge of the central cavity. Forced air circulation kept the temperature inside the cavity uniform and also eliminated to a large extent the necessity of defrosting the refrigerator. The compressor for the refrigerator was located just below the paraffin shield and a thermostat maintained temperatures constant to within ± 1.5 °F. The temperature of the water or ice sample was measured by a copper-constantan thermocouple connected to a potentiometer.

Demineralized and deaired water was used in all the samples. Two aluminum cans, having diameters of 9.4 and 14.4 cm respectively, held the samples. These sizes permitted a range in B^2 values from 0.1 cm^{-2} to 0.8 cm^{-2} . Intermediate values of B^2 were obtained by varying the level of the water or ice in the cans. For pulsed measurements above 0°C . each sample was weighed. The height of the sample was calculated from the weight, the density of water at the given temperature, and the area of the can. Since the density of ice is not as well known, the height of each ice sample was measured directly. The weight of some samples was recorded to provide information on the density

-  - PARAFFIN
-  - BORATED PARAFFIN
-  - COOLING COILS

LEGEND

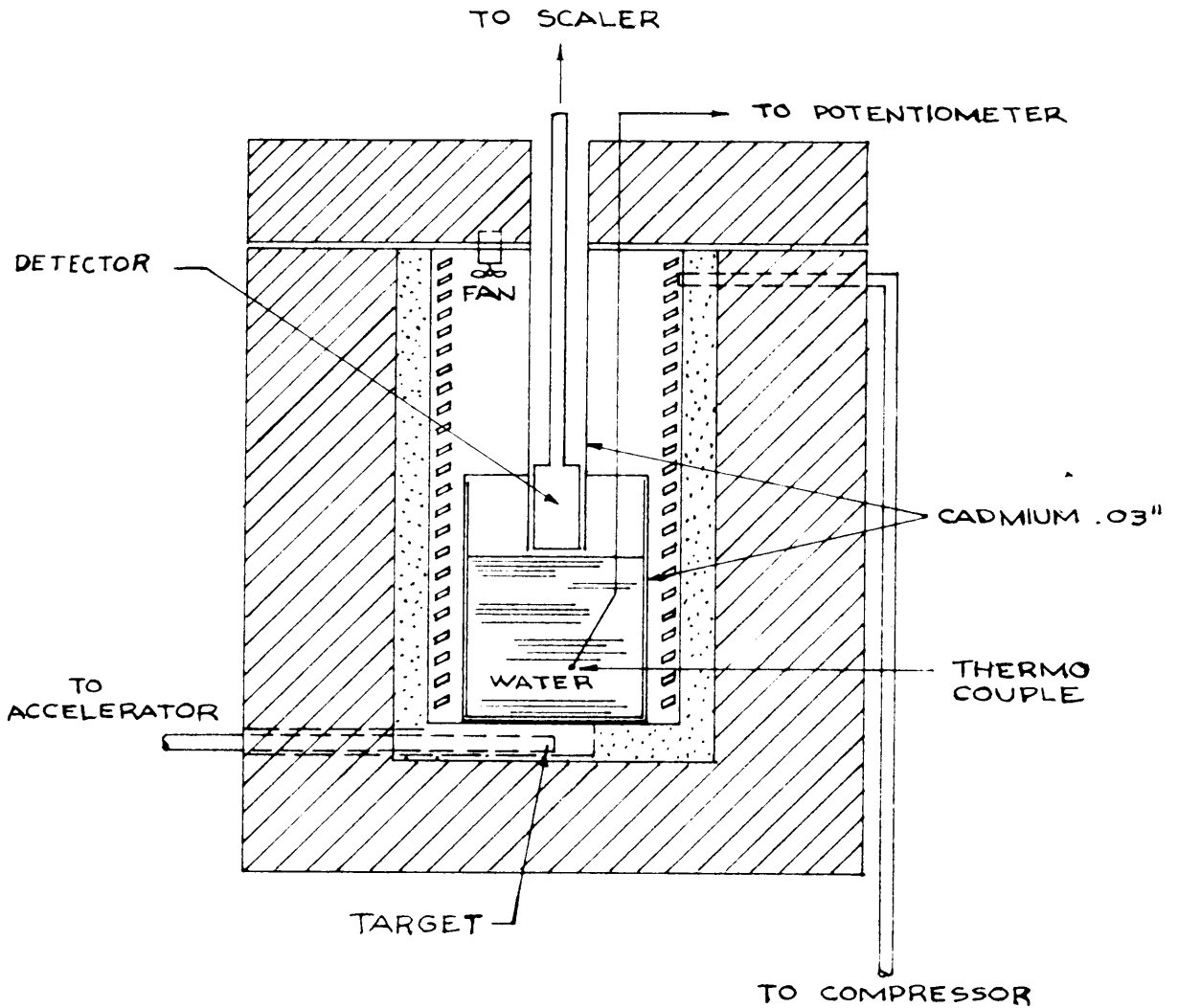


FIG. 5
EXPERIMENTAL ARRANGEMENT
NO SCALE

of ice. The average density of ice measured at -19°C . was $0.91 \pm .01$ gm/cm³. Barkov⁽¹⁰⁾ found a density of $0.89 \pm .01$ gm/cm³ for ice at -14°C .

The neutron source was located on the central axis beneath the cylindrical aluminum cans. A two inch N. Wood BF₃ detector, located on the central axis above the sample, counted the neutrons emerging from the surface. The detector was chosen for its high neutron and low gamma sensitivity. The radial surface of the detector was covered with a cadmium sleeve to restrict neutrons counted to those entering the end of the detector from the water or ice. This counter arrangement created a problem when measuring neutron lifetimes. A thermal neutron (0.025 ev) will travel at the rate of 0.22 centimeters per microsecond. A neutron counted after a long flight path will be erroneously recorded in a later time channel.

A technique was used to effectively shorten the detector to two inches in length and correct for long transit times of neutrons traveling axially. Sufficient B¹⁰ powder was placed in an aluminum sandwich to approximate the absorption of a two inch length of the BF₃ counter. Then two pulsed runs were made; one without the B¹⁰ sandwich and the end of the BF₃ detector at the surface of the water, and a second with the detector pulled back two inches inside the cadmium sleeve and the B¹⁰ sandwich over the end next to the water surface. The two inches of additional effective counter length on the second pulsed run made little contribution to the neutron count, and no correction was made.

The two pulsed runs were normalized to the same number of neutrons by a second BF_3 detector mounted in a fixed location directly beneath the paraffin shield. The decay curve one would measure with a counter two inches in length is obtained by subtracting the curves from the two pulsed runs.

Because of the relatively fast decay time for a burst of fast neutrons in light water, a repetition rate of 1000 cycles per second was used for the reference pulses. The delay time between the reference pulse and the opening of the first time channel was 100 microseconds. Channel widths of nominally 20 microseconds each were available using the converter in (Fig.2). Due to variations within the beam switching tubes controlling the channel widths, a small amount of variation was observed in the measured channel widths. Therefore, periodic channel width measurements were made while the experiment was in progress. The data from pulsed runs were corrected to the proper values for 20 microsecond channel widths by dividing the count in each channel by the respective measured channel width and then multiplying by 20.

D. Data Analysis

A high neutron background was present during all the pulsed runs. Measurements indicated the background was at most only slowly varying, but changed with sample size. A method of data analysis suggested by de Saussure and Silver⁽¹⁵⁾ eliminated the effect of the background without its exact value being known. The difference curve from the two pulsed runs was assumed to be composed of a simple exponential and a constant or slowly varying background. Points on the curve are then given by

$$N(t) = N_0 e^{-\alpha t} + b \quad (1)$$

where $N(t)$ = the number of counts in time interval Δt containing t .

α = the decay constant

b = the number of background counts

N_0 = the number of counts at $t = 0$.

If one divides the time into intervals of equal length, such that

$$t_k = (k - 1/2) \tau \quad k = 1, 2, 3, \dots \quad (2)$$

where t_k is the time at the center of the k th interval and τ = the length of the interval,

then

$$N_k = N_0 e^{-\alpha t_k} + b \quad (3)$$

where N_k is the number of counts in the k th interval

and

$$N_{k+1} = N_0 e^{-\alpha t_{k+1}} + b \quad (4)$$

Subtracting Eq. 4 from Eq. 3

$$N_k - N_{k+1} = N_0 \left[e^{-\alpha t_k} - e^{-\alpha t_{k+1}} \right] . \quad (5)$$

Substituting Eq. 2 into Eq. 5, one obtains

$$N_k - N_{k+1} = N_0 \left[e^{-\alpha(k-\frac{1}{2})\tau} - e^{-\alpha(k+\frac{1}{2})\tau} \right] ,$$

or

$$N_k - N_{k+1} = N_0 e^{-\alpha(k-\frac{1}{2})\tau} \left[1 - e^{-\alpha\tau} \right] . \quad (6)$$

For any given α , $1 - e^{-\alpha\tau}$ is a constant. Therefore, let

$$A = N_0 \left(1 - e^{-\alpha\tau} \right) .$$

Eq. 6 becomes

$$N_k - N_{k+1} = A e^{-\alpha t_k} ,$$

$$\ln (N_k - N_{k+1}) = \ln A - \alpha t_k$$

A plot of $N_k - N_{k+1}$ against t_k on semi-log graph paper will give a straight line whose slope is α . The linear portion of the decay curve was determined from the graph. The points along that portion were fitted to a straight line by the method of least squares to find the value of α .

E. Calculation of B^2

In order to analyse the results of pulsed neutron measurements according to Nelkin's prescription (Appendix), an appropriate B^2 value must be assigned to each sample. For simple geometric shapes, the B^2 value can be calculated from the eigenvalues of the equation

$$\nabla^2 \phi(\vec{r}) + B^2 \phi(\vec{r}) = 0 \quad (7)$$

where $\phi(\vec{r})$ is the spatially dependent neutron flux. The flux $\phi(\vec{r})$ is assumed to vanish at some distance ϵ beyond the actual physical boundary of the medium. The first eigenvalue of Eq. 7 for cylindrical geometry is

$$B^2 = \left[\frac{2.405}{R + \epsilon} \right]^2 + \left[\frac{\pi}{H + 2\epsilon} \right]^2, \quad (8)$$

where R and H are the radius and height of the cylinder, respectively, and 2.405 is the first zero of the J_0 Bessel Function.

The distance ϵ is known as the extrapolation distance since it is the distance from the edge to the point outside the cylinder where the asymptotic neutron flux would go through zero if the flux were represented in the region outside the medium by the same equation as inside the medium. Its value can be calculated explicitly for the one velocity Milne problem⁽²⁷⁾ where neutrons are diffusing across a plane interface between an infinite medium and a vacuum. A vacuum has the property that any neutron which enters it never returns to the medium. The vacuum therefore is equivalent to a perfectly absorbing medium. In an actual experiment one approximates a vacuum interface by covering

the outside surfaces of the diffusing medium with cadmium. For isotropic scattering in weak absorbers

$$\sum_s \epsilon = 0.71 \quad (9)$$

where \sum_s is the macroscopic scattering cross section. For the anisotropic scattering case with weak absorption

$$\sum_{tr} \epsilon = 0.71 \quad \text{or} \quad \epsilon = 0.71 \lambda_{tr} \quad (10)$$

where $\frac{1}{\sum_{tr}} = \lambda_{tr}$ the transport mean free path.

$$\sum_{tr} \approx \sum_s (1 - \bar{\mu}) \quad \text{where } \bar{\mu} = \text{average neutron scattering angle in lab system}$$

Although Eq. 10 does not strictly apply to small systems, it has often been used in lieu of anything better; for instance, see (5), (7), and (9). Assuming Eq. 10 for small geometries is reasonably justified if the transport cross section is not a strong function of energy. However, even for the case of water, where the transport cross section does depend on energy, Sjöstrand(19) has found that the deviations from Eq. 10 for slab geometry were small even for slabs 2-3 cm thick. His results were based on a calculation of the extrapolation distance for an infinite slab(21) using the P_3 approximation of the spherical harmonics method. In the first approximation, the dependence of the extrapolation distance on B^2 was found to be

$$\frac{\epsilon}{\lambda_{tr}} = 0.7051 \left[1 - B^2 \lambda_{tr}^2 (.0256 - .2825 b_1 + .0893 b_1^2) \right], \quad (11)$$

where the b's are the coefficients in the expansion of the scattering function into Legendre Polynomials, $P_n(\Omega' \cdot \Omega)$. viz.,

$$f(\Omega' \rightarrow \Omega) = \frac{1}{4\pi} \sum_{n=0}^{\infty} (2n+1) b_n P_n(\Omega' \cdot \Omega) \quad (12)$$

The scattering function $f(\Omega' \rightarrow \Omega)$ is the probability that a neutron with its velocity directed along Ω' will have its velocity directed along Ω after undergoing a scattering collision. In the derivation of Eq. 11, all $b_n > 1 = 0$.

A multigroup calculation of ϵ for an infinite slab by Gelbard and Davis⁽²⁸⁾ and a calculation also by Nelkin⁽⁴⁾ indicate that in the limit as $B^2 \rightarrow 0$

$$\epsilon \simeq 0.76 \lambda_{tr} \quad (13)$$

Nelkin states that while slab geometry can be handled satisfactorily by the method of Gelbard and Davis, the extension to an inherently three dimensional problem such as a small right circular cylinder is not very satisfactory because of the difficulty in calculating the corrections to the extrapolation distance.

A recent measurement of the extrapolation length in pulsed water systems has been made by DeJuren⁽²³⁾ for cylindrical geometry. His results are consistent with an extrapolation length of 0.4 cm for all cases. Campbell and Stelson⁽²⁴⁾ have also obtained an extrapolation distance of the same order of magnitude for pulsed water measurements. For both three inch and eight inch diameter cylinders they obtained an extrapolation distance of $0.45 \pm .05$ cm.

The extrapolation distance for hydrogen containing moderators varies with the neutron energy through the transport cross section. Deutsch⁽²⁵⁾ shows that for a Maxwellian neutron spectrum, the assumption of a $1/v$ energy dependence for the transport cross section is consistent

with the results of diffusion length measurements in water. The extrapolation distance would then vary as

$$\epsilon \propto E^{\frac{1}{2}} \quad \text{or} \quad \epsilon \propto T^{\frac{1}{2}} \quad (14)$$

where T is the temperature of the moderator in °K.

In view of the difficulty of calculating the proper extrapolation distance for a right circular cylinder, Eq. 10 was assumed for calculation of B^2 in this experiment. The value of λ_{tr} at room temperature used in calculating ϵ was the average of those given in Tables I and II. Then Eq. 10 becomes

$$\epsilon = 0.71 \lambda_{tr} = 0.31 \text{ cm} \quad (15)$$

which is nearly the same value as that used by Beyster (see Table I). Eq. 14 was used to find the extrapolation distance as a function of temperature.

III. REVIEW OF LITERATURE

A comprehensive summary of the measured neutron diffusion parameters in light water at 22°C. has been given by Kùchle⁽⁷⁾. Table I lists values of $(\sum_a v)$, D_0 , and C (see Appendix for definitions of coefficients) for water at room temperature. Kùchle⁽⁷⁾ has measured the diffusion parameters of water between 22 and 80°C. His results are shown in Table II.

Beckurts⁽¹⁷⁾ gives the following expression as representing the temperature dependence of the coefficient D_0 between 22 and 80°C:

$$D_0 = (134 \pm 7)T - (4700 \pm 2000) \text{ cm}^2/\text{sec} \quad (16)$$

where T is in °K.

Von Dardel and Sjöstrand⁽⁵⁾ found a value of $(2.4 \pm 0.4) \times 10^{-3}$ per °C. for the temperature dependence of the diffusion coefficient D_0 in the range 10 to 35°C.

The results of measurements of the coefficient D_0 made by Dio and Schopper⁽²⁾ in water over the temperature range 19 to 35°C. are shown below.

Temperature °C.	$D_0 \text{ cm}^2/\text{sec}$
19	35050 ± 600
49	38550 ± 1000
75	42250 ± 1000

Table I

Neutron Diffusion Parameters in Water at 22°C.

Source	$\sum_a v$ sec ⁻¹	D_0 cm ² /sec	C cm ⁴ /sec	λ_{tr} cm
Scott (33)	4695 ± 88	38500 ± 800		0.464 ± .010
Von Dardel & Sjöstrand (5)	4892 ± 48	36340 ± 750	7300 ± 1500	0.438 ± .010
Bracci & Coceva (32)	4950 ± 149	34850 ± 1100	3000 ± 1000	0.420 ± .013
Campbell & Stelson (1)	4808	34800	≈ 0	$\epsilon = .45 \pm .05$ cm
Beckurts (17)	4850 ± 150	34820 ± 720	3650 ± 400	
Beyster (20)	4768 ± 24	37503 ± 366	5116 ± 776	$\epsilon = .32$ cm

Table II

Neutron Diffusion Parameters in Water - Kühle (7)

Temperature °C.	$\sum_a v$ sec ⁻¹	D_0 cm ² /sec	C cm ⁴ /sec	λ_{tr} cm
22	4780 ± 80	35400 ± 400	4200 ± 500	0.427 ± .005
40	4820 ± 60	36300 ± 400	3300 ± 500	0.428 ± .005
60	4640 ± 80	40500 ± 500	5500 ± 500	0.453 ± .005
80	4660 ± 140	43100 ± 800	5800 ± 1000	0.463 ± .009

they derived an expression for temperature dependence of D_0 which is as follows:

$$D_0 = 35050 + (T - 19) (130 \pm 30) \text{ cm}^2/\text{sec} \quad (17)$$

where T is in °C.

Antonov⁽¹²⁾ reported the diffusion parameters of water measured at 23°C. and 80°C. as

Temp. °C.	$\sum_a v \text{ sec}^{-1}$	$D_0 \text{ cm}^2/\text{sec}$	$C \text{ cm}^4/\text{sec}$
23	4830 ± 140	35000 ± 1000	4000 ± 1000
80	4720 ± 133	$45000 \begin{matrix} + 4000 \\ - 2000 \end{matrix}$	$13000 \begin{matrix} + 5000 \\ - 7000 \end{matrix}$

In a later paper, Antonov⁽⁹⁾ reported the results of his pulsed measurements in water over the temperature range 0.5 to 286°C. Also one measurement was made in ice at -196°C. The diffusion parameters published in this paper are summarized in Table III.

A measurement of the diffusion length L of thermal neutrons in ice at -14°C. by Barkov⁽¹⁰⁾ resulted in a value of $L = 2.85 \pm 0.05$ cm. He shows that the magnitude of L at -14°C in ice can be deduced from that of water by correcting for the lower density and temperature of ice which implies that the difference in chemical binding between ice and water has little effect on the diffusion length. From Eq. 18 (below) the value of the diffusion coefficient at -14°C. calculated from the diffusion length is

$$D_0 = 35100 \pm 1000 \text{ cm}^2/\text{sec}.$$

Table III

Neutron Diffusion Parameters in Water - Antonov⁽¹²⁾

Temp °C	$\sum_a v$ sec ⁻¹	D_0 cm ² /sec	C cm ⁴ /sec
0.5	4878 ± 300	32310 ± 1390	4000 ± 1900
3	4830 ± 290	33725 ± 1420	4400 ± 1900
7	4926 ± 300	33370 ± 1435	3600 ± 1500
21	4830 ± 290	36210 ± 1485	4000 ± 1900
71	4695 ± 277	43310 ± 1860	4800 ± 2000
98	4425 ± 280	47570 ± 1950	7200 ± 3000
105	4525 ± 260	48280 ± 1980	5200 ± 2400
136	4525 ± 260	53250 ± 2340	6000 ± 2500
138	4348 ± 270	54315 ± 2336	8800 ± 3900
159	4566 ± 260	57865 ± 2430	8000 ± 3400
200	4310 ± 267	68160 ± 2860	9600 ± 3900
250	3861 ± 222	80585 ± 3390	11600 ± 4800
286	3584 ± 220	96560 ± 3960	20000 ± 8300
-196	4505	10500 ± 400	2500 ± 1000

$$\lambda_{tr} (-196^\circ\text{C}) = 0.248 \pm .010 \text{ cm}$$

Wright⁽²⁶⁾ has made measurements of the diffusion length of thermal neutrons in water at three temperatures. The corresponding diffusion coefficient was calculated from his measured diffusion length by Eq. 18.

Temperature °C.	L cm	D ₀ cm ² /sec (calc.)
25	2.714 ± .010	34800 ± 650
190	3.927 ± .023	64200 ± 1200
277	5.360 ± .037	104000 ± 2000

The value of D₀ can be calculated from the diffusion length L by setting the decay constant α from pulsed neutron theory (see Eq. 28, Appendix) equal to zero, corresponding to a steady state system. For a stationary neutron population (α = 0), the equation:

$$\alpha = \alpha_0 + D_0 B^2 - CB^4 \quad (\text{Eq. 28, Appendix})$$

becomes

$$\alpha_0 + D_0 B^2 - CB^4 = 0$$

but $B = 1/iL$ (18, 19) where $i = \sqrt{-1} \Rightarrow$

$$\alpha_0 - D_0/L^2 - C/L^4 = 0$$

$$\therefore D_0 = L^2 \alpha_0 - C/L^2 \quad (18)$$

The value of α₀ is assumed to be independent of temperature for a 1/v absorber (such as water approximates) except for density effects.

Beckurts⁽¹⁷⁾ does not give any temperature dependence for the diffusion cooling coefficient but states that the ratio of D₀²/C is

constant and equal to $3.4 \times 10^5 \text{ sec}^{-1}$.

A theoretical calculation of the thermal neutron diffusion properties of water at room temperature carried out by Nelkin⁽³⁾ gave the following values:

$$D_0 = 37900 \text{ cm}^2 / \text{sec}$$

$$C = 3000 \text{ cm}^4 / \text{sec}$$

$$\frac{d (\ln D_0)}{dT} = .0034 \tag{19}$$

Nelkin's theory predicted that $(\ln D_0)$ should have a linear temperature dependence rather than D_0 itself.

It is apparent that the results of measurements of the diffusion parameters in light water are not in good agreement. There is a need for some very careful measurements over the whole temperature range. One such measurement has been made by Lopez and Beyster⁽²⁰⁾ at 26.7°C . using the high intensity pulsed linear electron accelerator at General Atomics. They also discuss possible sources of error in earlier measurements. Their results are included in Table I.

The temperature dependence of D_0 and C are shown in Figs. 6 and 7, respectively. The solid line in Fig. 6 is the theoretical temperature dependence of D_0 predicted by Nelkin⁽³⁾ (Eq. 19). The fit is quite good, considering the assumptions made in the derivation of Eq. 19. No direct prediction of the dependence of C upon temperature has been made. If, however, one assumes the ratio of D_0^2/C to be constant over a range of temperatures; from Eq. 19 the temperature dependence of C

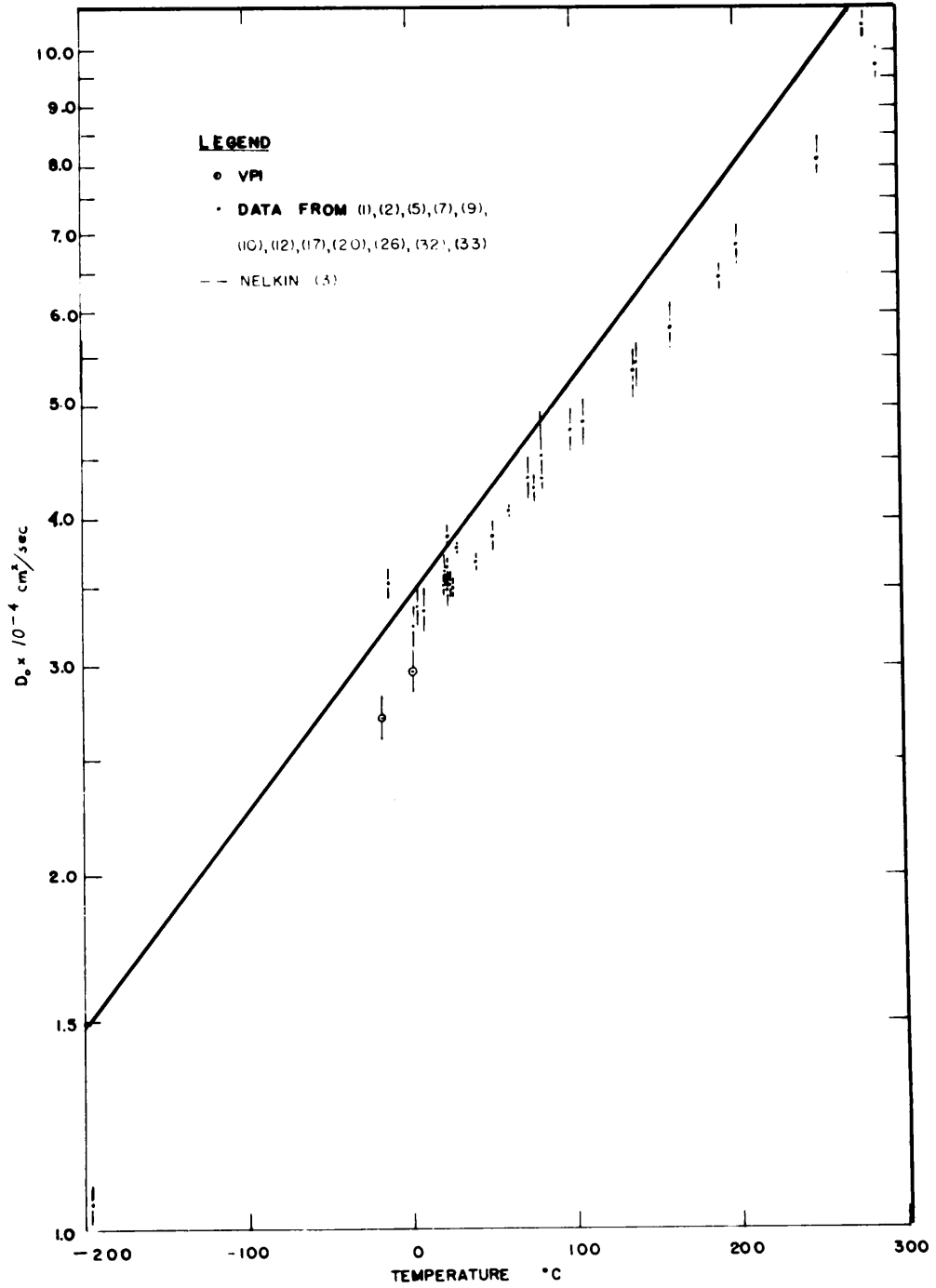


FIG. 6 TEMPERATURE DEPENDENCE OF THE DIFFUSION COEFFICIENT D_0 .

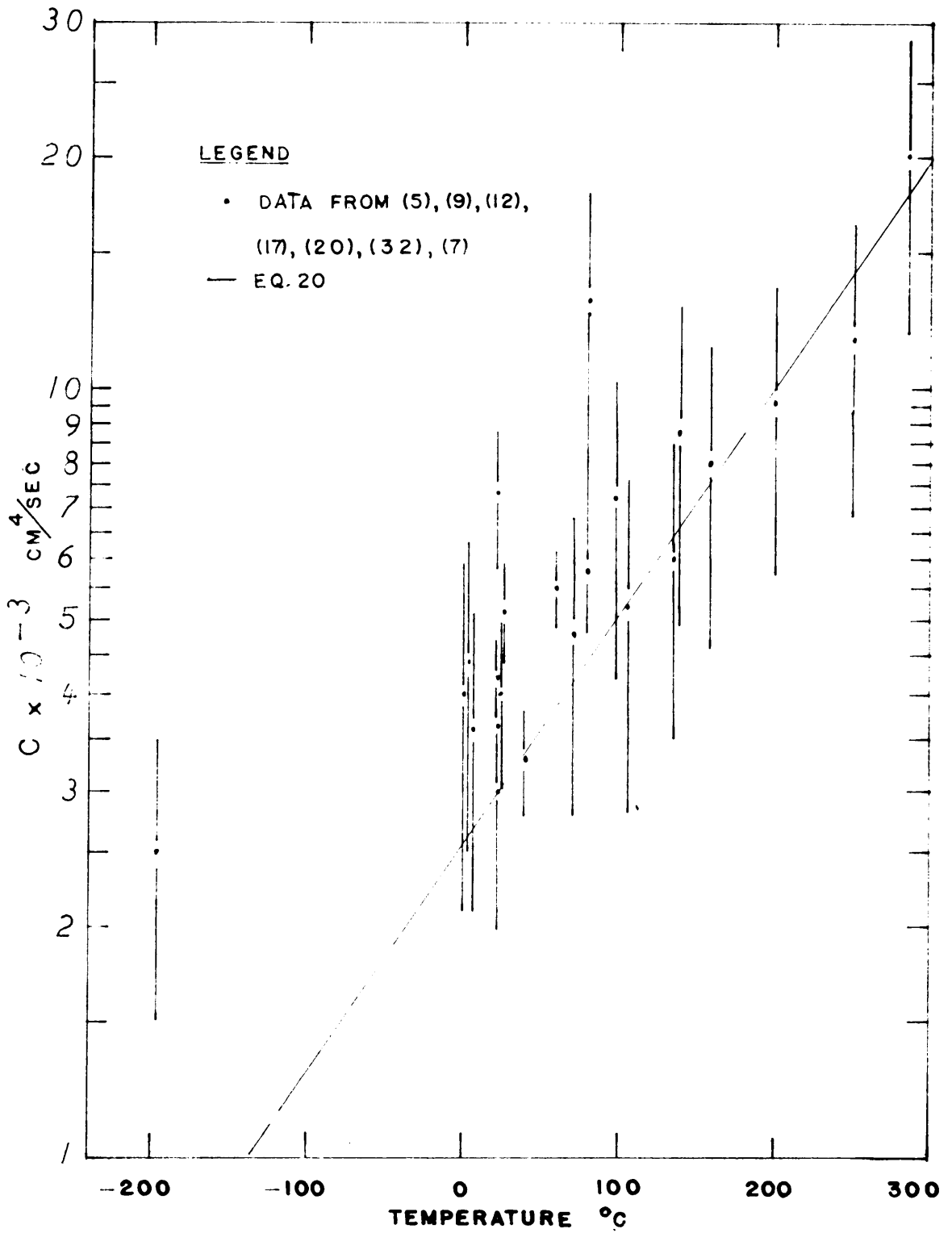


FIG. 7 TEMPERATURE DEPENDENCE OF DIFFUSION COOLING COEFFICIENT C

becomes

$$D_o^2 = 3.4 \times 10^5 C.$$

$$2 \ln D_o = \ln 3.4 \times 10^5 + \ln C$$

$$2 \frac{d(\ln D_o)}{dT} = \frac{d(\ln C)}{dT} .$$

By Eq. 19

$$\frac{d(\ln C)}{dT} = 2(.0034) = .0068 \quad (20)$$

with C (22°C) = 3000 cm⁴/sec.

Eq. 20 is plotted as the solid line in Fig. 7.

IV. RESULTS AND DISCUSSION

A. Results of Measurements

Pulsed neutron measurements were carried out in light water at two temperatures, viz., $1.0 \pm 1.0^{\circ}\text{C}$. and $-19 \pm 1.0^{\circ}\text{C}$. A few measurements were made at 25°C . to check the equipment. The decay constants measured at room temperature agreed with values reported in the literature. For the two lower temperatures the size of each sample, its B^2 value calculated from Eq. 12 and 14, and measured decay constant are shown in Tables IV and V. When more than one measurement of the decay constant was made for a given sample the recorded value is the average of the measured values.

The measured decay constants were fitted by the method of least squares to a polynomial in B^2 in accordance with the theory given in the Appendix. A linear and then a quadratic functional dependence of α upon B^2 was assumed. The value of $(\sum a v)$, the intercept at $B^2 = 0$, can be calculated for each temperature as it is temperature independent except for density effects. The calculated intercept was used to improve the estimates of the polynomial coefficients since data was lacking for low values of B^2 . Kuchle⁽⁷⁾ has used a similar procedure in the analysis of his data. The decay constants for water at 1.0°C . are shown as a function of B^2 in Fig. 8; those for ice at -19°C . in Fig. 9. The solid line in each figure is the graph of the equation from the least squares fit to a linear relation. The diffusion coefficients for water found in this experiment are given in Table VI.

Table IV

Decay Constants Measured at 1.0°C.

H cm.	R cm.	$B^2 \text{ cm}^{-2}$	$\alpha \text{ sec}^{-1}$
13.90	7.2	0.150 ± .001	9056 ± 300
7.64	7.2	0.249 ± .002	11080 ± 450
6.51	7.2	0.299 ± .003	12670 ± 500
5.74	7.2	0.350 ± .005	13120 ± 550
5.23	7.2	0.395 ± .006	17400 ± 500
4.98	7.2	0.422 ± .007	16770 ± 450
4.63	7.2	0.467 ± .008	19080 ± 500
4.31	7.2	0.516 ± .009	20120 ± 500
3.99	7.2	0.576 ± .012	23690 ± 700
4.30	4.7	0.647 ± .014	24030 ± 800
3.90	4.7	0.725 ± .016	25670 ± 900
3.63	4.7	0.790 ± .018	27060 ± 1000

Table V

Decay Constants Measured at -19°C.

H cm	R cm	$B^2 \text{ cm}^{-2}$	$\alpha \text{ sec}^{-1}$
14.3	7.2	0.148 ± .001	9256 ± 300
8.1	7.2	0.235 ± .002	9990 ± 700
6.3	7.2	0.313 ± .003	12045 ± 500
5.6	7.2	0.363 ± .005	13640 ± 600
5.0	7.2	0.422 ± .007	16200 ± 500
4.45	7.2	0.496 ± .009	18770 ± 800
5.45	4.7	0.506 ± .008	19130 ± 500
4.3	7.2	0.521 ± .011	17720 ± 400
3.9	7.2	0.599 ± .013	19880 ± 950
4.2	4.7	0.669 ± .015	22330 ± 600
3.8	4.7	0.752 ± .017	24850 ± 1000

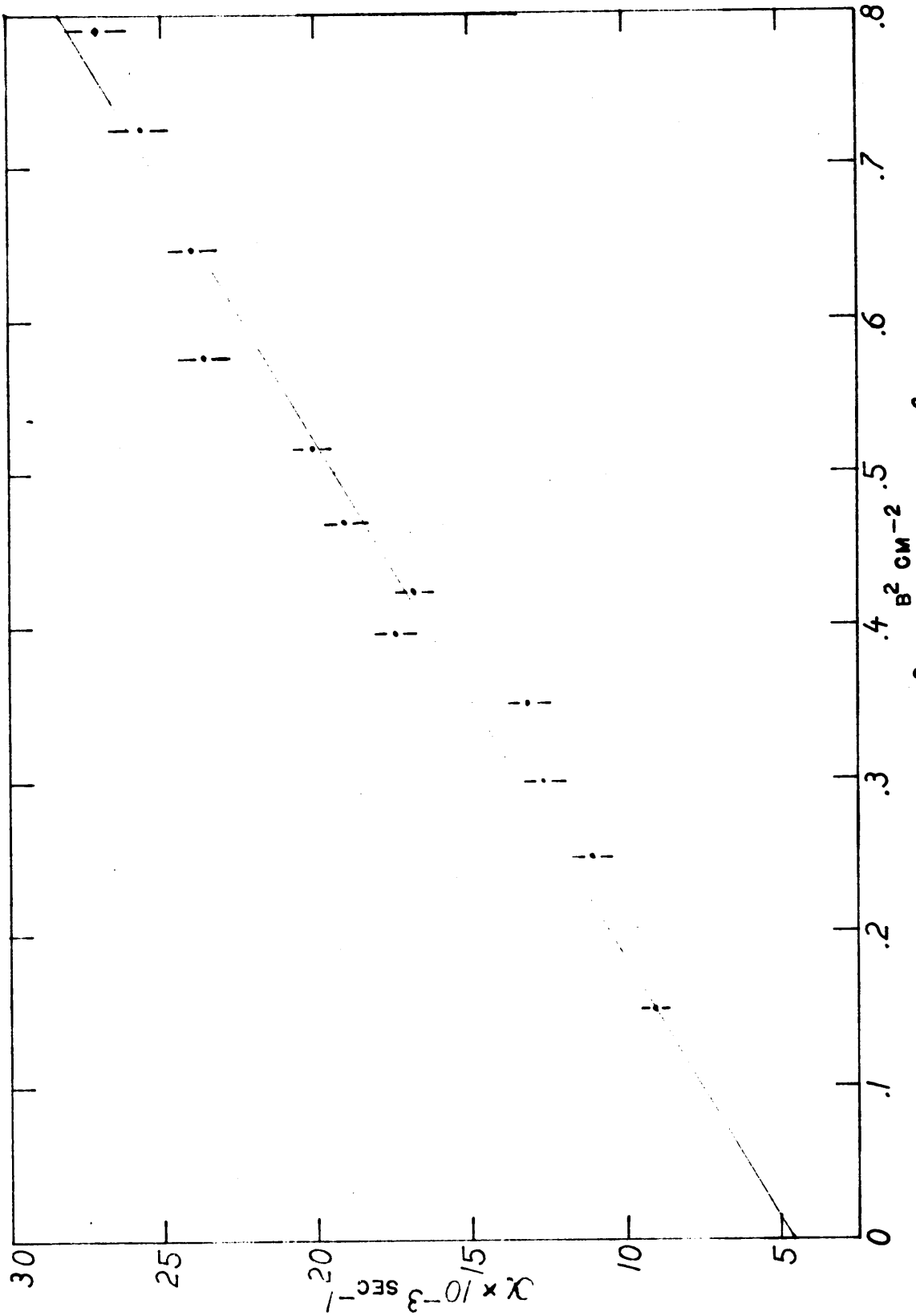


FIG. 8 DECAY CONSTANTS AS A FUNCTION OF B^2 FOR WATER AT 1 °C.

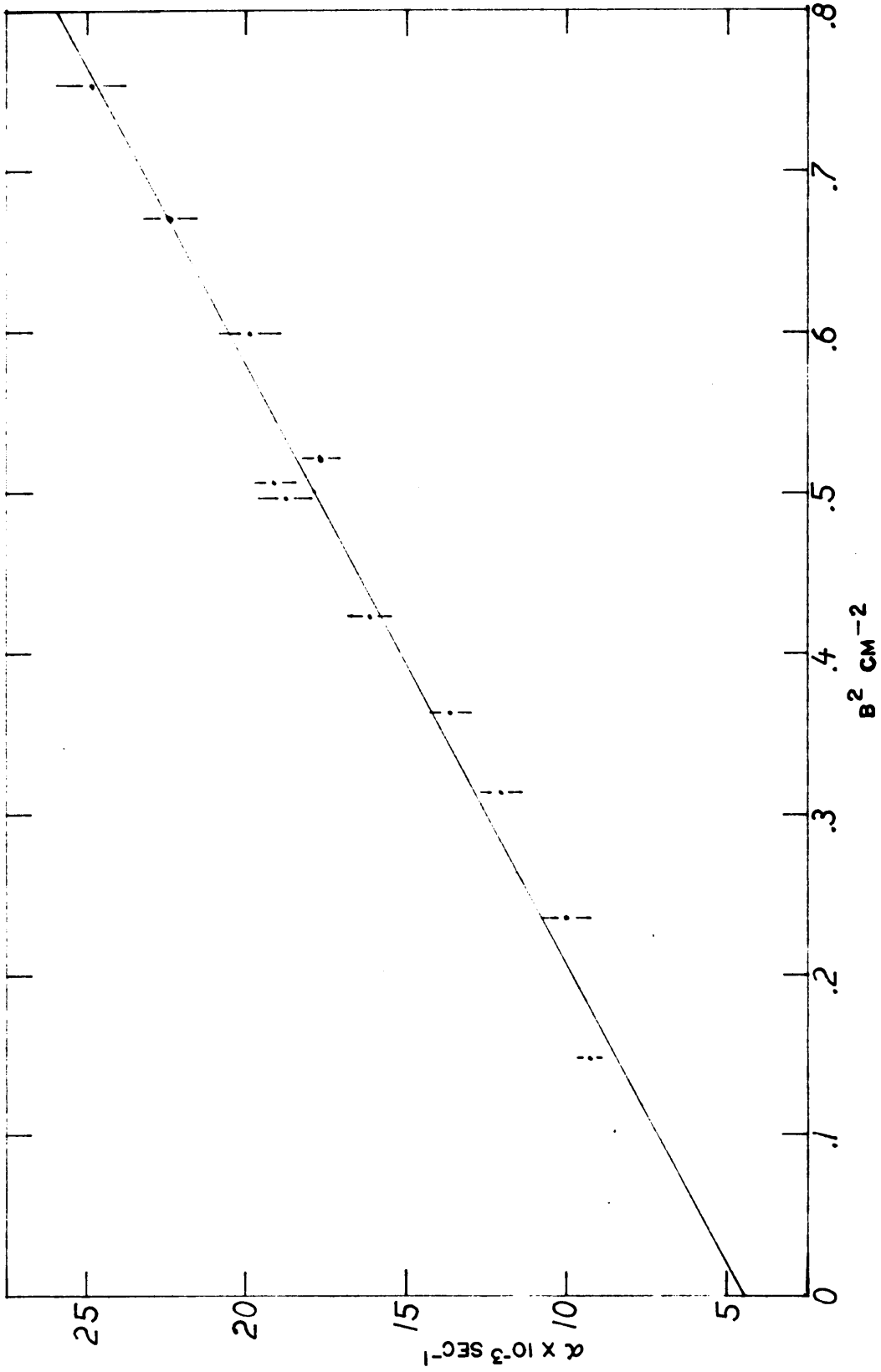


FIG. 9 DECAY CONSTANTS AS A FUNCTION OF B^2 FOR ICE AT -19°C .

The criterion used to decide which functional form gave the better fit to the data, following Parratt(29), is:

$$\beta = \frac{\sum_{i=1}^N (\alpha_i - \alpha_i^*)^2}{N - A^*} \quad (21)$$

where α_i = the measured value of the decay constant at B_i^2
 α_i^* = value of decay constant at B_i^2 calculated from functional form

N = number of measurements

A^* = number of constants in function.

The relation which gives the smaller value of β is the better fit to the data. The values of β calculated from Eq. 21 for the above assumed functional dependence of α on B^2 are as follows:

Temp.	functional form	Comparison Factor β
1°C.	linear	858,155
	quadratic	924,129
-19°C.	linear	431,311
	quadratic	466,120

The linear fit in each case gave a slightly smaller β value. A quadratic, therefore, does not fit the data better than a linear relation. This also follows from the errors in the coefficients of the B^4 term in the quadratic relation which in each case are larger than the coefficients themselves. The data from this experiment were not sufficiently precise to permit a determination of the diffusion cooling coefficient.

Table VI

Diffusion Coefficients of Water from this Experiment

Temperature $1.0 \pm 1.0^\circ\text{C}$.

functional form	$(\sum a^2 v) \text{sec}^{-1}$	$D_0 \text{ cm}^2/\text{sec}$	$C \text{ cm}^4/\text{sec}$
linear	4595 ± 365	29600 ± 840	
quadratic	4590 ± 417	29670 ± 2640	92 ± 3550

Temperature $-19 \pm 1.0^\circ\text{C}$.

linear	4355 ± 263	27050 ± 630	
quadratic	4380 ± 294	26680 ± 2060	-570 ± 2980

B. Sources of Error

The largest source of error in the measurements of the decay constants was the large neutron background mentioned previously (section II-D), which was present during all the pulsed runs. The neutron decay could be followed for approximately one order of magnitude before reaching the background. A better estimate of the equilibrium decay constant could be obtained if the background were reduced. The errors associated with the decay constants given in Tables IV and V were assigned from the reproducibility of the data.

The error in the B^2 values is from three main sources. First, the aluminum cans holding the samples were not perfect right circular cylinders, but had the lower corner rounded. However, the radius of curvature was small. A more important source of error was in determining the exact height of the sample, especially for the ice measurements, since the top surface of the ice was never perfectly flat. The height was averaged from measurements in several places. The third source of error was discussed earlier in selecting the extrapolation distance. These errors in B^2 are additive in their effect.

The errors in the diffusion coefficients in Table VI are statistical errors calculated by the method given by Parratt (29).

V. ACKNOWLEDGEMENTS

The author wishes to express his thanks to the following people who have assisted in this investigation: To Dr. Andrew Robeson and Dr. Keith Furr for their help and guidance; to Mr. Barnett for his help in the machine shop; to Mr. Newmire for his assistance with electronic problems; to Messrs. Bowden, Jalbert, and Foster for their assistance in writing and running the computer program; to George

for the meticulous drawings; to Lee and William

for their help in the construction and operation of the accelerator; to Burroughs Corporation for information on their beam switching tubes; and to Mrs. Mary Krummell for typing this manuscript.

The author also wishes to express his appreciation for financial support of this research to the following sources: Special Fellowship in Nuclear Science and Engineering (U.S.A.E.C.), Atomic Energy Commission Contract No. and the Virginia Polytechnic Institute Engineering Experiment Station.

VI. BIBLIOGRAPHY

1. Campbell, E. C. and Stelson, P. H., "Experiments With a Pulsed-Neutron Source", ORNL-2076, 10 September 1956, p. 32
2. Dio, W. H. and Schopper, E., "Temperature Dependence of the Diffusion Coefficient and the Diffusion Length of Thermal Neutrons in Water", Nuclear Physics Vol. 6, March-May 1958, p. 175
3. Nelkin, M., "Scattering of Slow Neutrons by Water", Physical Review Vol. 119, 15 July 1960, p. 741
4. Nelkin, M., "The Decay of a Thermalized Neutron Pulse," Nuclear Science and Engineering Vol. 7, 1960, p. 210
5. Von Dardel, G. and Sjöstrand, N. G., "Diffusion Parameters of Thermal Neutrons in Water", Physical Review Vol. 96 Part 2, 15 November - 15 December 1954, p. 1245
6. Beckurts, K. H., "Reactor Physics Research With Pulsed Neutron Sources", Nuclear Instruments and Methods Vol. 11, January 1961, p. 144
7. Kühle, M. "Measurement of the Temperature Dependence of Neutron Diffusion in Water and Diphenyl by the Impulse Method", Nukleonik, Vol. 2, June 1960, p. 131
8. De Coulon, G. and Zweifel, P. F., "Note on the Thermal Neutron Spectrum in a Diffusing Medium", Nuclear Science and Engineering Vol. 5, 1959, p. 203

9. Antonov, A. V., et al., "A Study of Neutron Diffusion in Beryllium, Graphite, and Water by the Impulse Method", Proceedings of the International Conference on the Peaceful Uses of Atomic Energy Vol. 5, 1955, p. 3
10. Barkov, L. M., "Measurement of the Diffusion Length of Thermal Neutrons in Ice", Journal of Nuclear Energy Vol. 8, July 1960, p. 102
11. Oak Ridge National Laboratory, "Radioisotopes Catalog" 3rd Revision, May 1960, p. 185
12. Antonov, A. V., et al., "Study of the Diffusion and Thermalization of Neutrons in Water and Ice within a Wide Range of Temperatures, Using the Impulse Method", Proceedings of the Symposium on Inelastic Scattering on Neutrons in Solids and Liquids, Vienna, 1960
13. Morris, J. R., "A Pulsed Ion Source for a 250 Kev Cockcroft-Walton Accelerator", M. S. Thesis - Virginia Polytechnic Institute, 1959
14. Hollandsworth, C. E., "The Design and Construction of a One Megacycle Frequency Divider", M. S. Thesis - Virginia Polytechnic Institute, 1961
15. DeSaussure, G. and Silver, E. G., "Determination of the Neutron Diffusion Parameters in Room Temperature Beryllium", ORNL-2641, 27 February 1959

16. Higginbotham, W. A. and Rankowitz, S., "A Combined Current Indicator and Integrator", Reviews of Scientific Instruments Vol. 22 No. 9, September 1951, p. 683
17. Beckurts, K. H., "Work With the Karlsruhe Pulsed Sources", UCRL-5665, December 1958, p. 42
18. Davison, B., "Neutron Transport Theory", Oxford University Press, London, England, 1957, p. 55
19. Sjöstrand, N. G., "Recent Pulsed Work in Sweden", UCRL-5665, December 1958, p. 36
20. Lopez, W. M. and Beyster, J. R., "Measurement of Neutron Diffusion Parameters in Water by the Pulsed Method", Nuclear Science and Engineering Vol. 12, 1962, p. 190
21. Sjöstrand, N. G., "On the Theory Underlying Diffusion Measurements With Pulsed Neutron Sources", Arkiv för Fysik Band 15 Häfte 2, 1959, p. 147
22. Hanson, A. O., Taschek, R. F., and Williams, J. H., "Monoenergetic Neutrons from Charged Particle Reactions", Reviews of Modern Physics Vol. 21, October 1949, p. 641
23. De Juren, J. A., Stooksberry, R., and Carrol, E. E., "Measurements of Extrapolation Lengths in Pulsed Water Systems", Paper presented at the Brookhaven Conference on Neutron Thermalization, May 1962
24. Campbell, E. C., Remark quoted from UCRL-5665, December 1958, p. 27

25. Deutsch, R. W., "Temperature Dependence of the Thermal Diffusion Length in Water", Nuclear Science and Engineering Vol. 1, 1956, p. 252
26. Wright, W. B. and Frost, R. T., "Preliminary Diffusion Length Measurements in Hot Water", (Abstract) KAPL-M-WBW-2, 31 October 1956
27. Weinberg, A. M. and Wigner, E. P., "The Physical Theory of Neutron Chain Reactors", The University of Chicago Press, Chicago, Ill., 1958, p. 264
28. Gelbard, E. M., and Davis, J. A., "The Behavior of Extrapolation Distances in Die-Away Experiments", Nuclear Science and Engineering Vol. 13, 1962, p. 237
29. Parratt, L. G., "Probability and Experimental Errors in Science", John Wiley and Sons, Inc., New York, N. Y., 1961, p. 134
30. Silver, E. G. and de Saussure, G., "Pulsed-Neutron Measurements in Beryllium", Annual Progress Report Neutron Physics Division ORNL-3193, 1 September 1961, p. 215
31. Virginia Polytechnic Institute Engineering Experiment Station Report. (To be published)
32. Bracci, A. and Coceva, C., Nuovo Cimento Vol. 4, Series X, 1956, p. 59 (Original not seen)
33. Scott, F. R., Thompson, D. B., and Wright, W., "Thermal Neutron Capture Cross Sections of Hydrogen, Boron, and Silver", Physical Review Vol. 95 Part 1, 15 July 1954, p. 582

**The vita has been removed from
the scanned document**

V. APPENDIX

Theory of Pulsed Neutron Measurements

Following the introduction of a burst of fast neutrons into a finite moderating sample, the thermalized neutrons reach an asymptotic state, known as the fundamental mode. The neutron density in the fundamental mode decays exponentially with a decay constant α .

A theoretical investigation of pulsed neutron experiments has been made by Nelkin⁽⁴⁾. The analysis is restricted to neutrons in an infinite medium which have reached the fundamental mode. The transport equation is solved by taking a Fourier Transform in the spatial variable. The decay constant α is expanded in powers of the Transform variable B . The infinite medium theory can be compared with a finite medium experiment by assigning an equivalent infinite medium B^2 value to each finite sample. The procedure for assigning the appropriate B^2 value to a finite sample is discussed in Section II-E.

The time dependent transport equation for neutrons in an infinite medium may be written as

$$\left[\frac{1}{v} \frac{\partial}{\partial t} + \mu \frac{\partial}{\partial z} + \Sigma_s(E) + \Sigma_a(E) \right] f(z, \mu, E, t) = S(z, \mu, E) \delta(t) + \frac{1}{2} \int_0^\infty dE' \Sigma_o(E' \rightarrow E) \int_{-1}^1 d\mu' f(z, \mu', E', t) \quad (1)$$

where

v = velocity of the neutrons

$\mu = \frac{\overline{\mathbf{v} \cdot \mathbf{z}}}{vz}$ = the cosine of the neutron scattering angle

$\Sigma_0(E' \rightarrow E)$ = the energy transfer cross section. $\int_0^\infty \Sigma_0(E' \rightarrow E) dE$ is the probability that a neutron of energy E' will have its energy in the interval dE containing E after undergoing a scattering collision.

$$\Sigma_s(E) = \int_0^\infty \Sigma_0(E \rightarrow E') dE' = \text{the macroscopic} \quad (2)$$

scattering cross section at E . The probability of scattering to any final neutron energy, E' , is considered.

$\Sigma_a(E)$ = the macroscopic absorption cross section at energy E

$E = \frac{1}{2} mv^2$ = energy of neutrons

$S(z, \mu, E)$ = neutron source term

$\delta(t)$ = Dirac delta function in time

$\delta(t) = 0$ for $t \neq 0$

$f(z, \mu, E, t) dV d\mu dE$ = the number of neutrons at time t in the volume element dV containing z , in the energy interval dE containing E , and whose directions of motion lie within the angular element $d\mu$ containing μ , multiplied by the speed of these neutrons.

Eq. 1 assumes spatial variation in one dimension only, no regeneration of neutrons, and isotropic scattering.

Assume a solution to Eq. 1, for $t > 0$, of the form

$$f(z, \mu, E, t) = f_\alpha(z, \mu, E) e^{-\alpha t} \quad (3)$$

where $f_\alpha(z, \mu, E)$ describes the time independent fundamental neutron distribution. A superposition of solutions of the form of Eq. 3 is necessary to satisfy the boundary conditions at $t = 0$. For a finite medium, the solutions form a discrete set.

Substituting Eq. 3 into Eq. 1 gives, for $t > 0$,

$$\left[\mu \frac{\partial}{\partial z} + \Sigma_s(E) + \Sigma_a(E) - \frac{\alpha}{v} \right] f_\alpha(z, \mu, E) = \frac{1}{2} \int_0^\infty dE' \Sigma_0(E' \rightarrow E) \int_{-1}^1 d\mu' f_\alpha(z, \mu', E'). \quad (4)$$

The source term vanishes for $t > 0$ because of the delta function at $t = 0$.

The solution to Eq. 4 is obtained by taking a Fourier Transform in the spatial variable. Define $\phi_\alpha(B, \mu, E)$ as the Fourier Transform of $f_\alpha(z, \mu, E)$, i.e.;

$$\phi_\alpha(B, \mu, E) = \int_{-\infty}^{\infty} e^{-iBz'} f_\alpha(z', \mu, E) dz' \quad (5)$$

where B is the Fourier Transform variable.

Multiplying Eq. 4 by e^{-iBz} and integrating over all z , one obtains

$$\begin{aligned} \int_{-\infty}^{\infty} e^{-iBz'} \left[\mu \frac{\partial}{\partial z'} + \Sigma_s(E) + \Sigma_a(E) - \frac{\alpha}{v} \right] f_\alpha(z', \mu, E) dz' = \\ \frac{1}{2} \int_{-\infty}^{\infty} dz' e^{-iBz'} \int_0^\infty dE' \Sigma_0(E' \rightarrow E) \int_{-1}^1 d\mu' f_\alpha(z', \mu', E'). \end{aligned} \quad (6)$$

The first term of Eq. 6 may be integrated by parts giving

$$\begin{aligned} \int_{-\infty}^{\infty} \mu e^{-iBz'} \frac{\partial}{\partial z'} f_\alpha(z', \mu, E) dz' = \mu e^{-iBz'} f_\alpha(z', \mu, E) \Big|_{-\infty}^{\infty} + \\ iB\mu \int_{-\infty}^{\infty} e^{-iBz'} f_\alpha(z', \mu, E) dz'. \end{aligned} \quad (7)$$

Since the neutron flux must vanish at both $+\infty$ and $-\infty$, the first term on the right side of Eq. 7 vanishes and Eq. 6 becomes

$$\left[\Sigma_s(E) + \Sigma_a(E) - \frac{\alpha}{v} + iB\mu \right] \int_{-\infty}^{\infty} e^{-iBz'} f_{\alpha}(z', \mu, E) dz' =$$

$$\frac{1}{2} \int_0^{\infty} dE' \Sigma_0(E' \rightarrow E) \int_{-1}^1 d\mu' \int_{-\infty}^{\infty} e^{-iBz'} f_{\alpha}(z', \mu', E') dz'.$$

(8)

Substituting Eq. 5 into Eq. 8 gives

$$\left[\Sigma_s(E) + \Sigma_a(E) - \frac{\alpha}{v} + iB\mu \right] \Phi_{\alpha}(B, \mu, E) =$$

$$\frac{1}{2} \int_0^{\infty} dE' \Sigma_0(E' \rightarrow E) \int_{-1}^1 d\mu' \Phi_{\alpha}(B, \mu', E').$$

(9)

Rewriting Eq. 9 and integrating over μ , one obtains

$$\int_{-1}^1 \Phi_{\alpha}(B, \mu'', E) d\mu'' =$$

$$\frac{1}{2} \int_{-1}^1 \frac{d\mu''}{\Sigma_s(E) + \Sigma_a(E) - \frac{\alpha}{v} + iB\mu''} \int_0^{\infty} dE' \Sigma_0(E' \rightarrow E) \int_{-1}^1 d\mu' \Phi_{\alpha}(B, \mu', E').$$

(10)

$$\int_{-1}^1 \phi_{\alpha}(B, \mu'', E) d\mu'' = \frac{1}{2iB} \ln \left[\frac{\Sigma_s(E) + \Sigma_a(E) - \frac{\alpha}{v} + iB}{\Sigma_s(E) + \Sigma_a(E) - \frac{\alpha}{v} - iB} \right] \int_0^{\infty} dE' \Sigma_o(E' \rightarrow E) \int_{-1}^1 d\mu' \phi_{\alpha}(B, \mu', E'). \quad (11)$$

From the definition of $\tan^{-1} z$, it can be shown that

$$\tan^{-1} z = \frac{1}{2i} \ln \left[\frac{1 + iz}{1 - iz} \right] \quad (12)$$

Define $\phi_{\alpha}(B, E)$ to be

$$\phi_{\alpha}(B, E) = \int_{-1}^1 \phi_{\alpha}(B, \mu', E) d\mu' \quad (13)$$

Substituting Eq. 12 and Eq. 13 into Eq. 11 gives

$$\phi_{\alpha}(B, E) = \left[\frac{1}{B} \tan^{-1} \frac{B}{\Sigma_s(E) + \Sigma_a(E) - \frac{\alpha}{v}} \right] \left[\int_0^{\infty} dE' \Sigma_o(E' \rightarrow E) \phi_{\alpha}(B, E') \right] \quad (14)$$

Define

$$g(B, \alpha, E) = \frac{1}{B} \tan^{-1} \frac{B}{\Sigma_s(E) + \Sigma_a(E) - \frac{\alpha}{v}} \quad (15)$$

Substituting Eq. 15 into Eq. 14 gives

$$\phi_{\alpha}(B, E) = g(B, \alpha, E) \int_0^{\infty} dE' \Sigma_o(E' \rightarrow E) \phi_{\alpha}(B, E') \quad (16)$$

The integral equation (Eq. 16) is considered an eigenvalue problem in the energy variable with eigenvalues and eigenfunctions depending on the variable B.

In order to illustrate the constraints on the problem, Eq. 16 is rewritten and $\Sigma_s(E) \phi_{\alpha}(B, E)$ subtracted from both sides.

$$\begin{aligned} \Phi_{\alpha}(B, E) \left[g(B, \alpha, E) \right]^{-1} - \Sigma_s(E) \Phi_{\alpha}(B, E) = \\ \int_0^{\infty} \Sigma_o(E' \rightarrow E) \Phi_{\alpha}(B, E') dE' - \Sigma_s(E) \Phi_{\alpha}(B, E) \end{aligned} \quad (17)$$

Writing Eq. 17 in operator notation

$$F(B, \alpha, E) \Phi_{\alpha}(B, E) = S \Phi_{\alpha}(B, E) \quad (18)$$

where

$$F(B, \alpha, E) = \left[g(B, \alpha, E) \right]^{-1} - \Sigma_s(E) \quad (19)$$

and

$$S \Phi_{\alpha}(B, E) = \int_0^{\infty} \Sigma_o(E' \rightarrow E) \Phi_{\alpha}(B, E') dE' - \Sigma_s(E) \Phi_{\alpha}(B, E) \quad (20)$$

Constraint 1, A statement of neutron conservation is obtained by integrating Eq. 18 over energy. The conservation condition is

$$\int_0^{\infty} F(B, \alpha, E) \Phi_{\alpha}(B, E) dE = 0 \quad (21)$$

since the integral of $S \Phi_{\alpha}(B, E)$ may be shown to vanish.

$$\int_0^{\infty} F(B, \alpha, E) \Phi_{\alpha}(B, E) dE = \int_0^{\infty} S \Phi_{\alpha}(B, E) dE$$

From Eq. 20

$$\int_0^{\infty} F(B, \alpha, E) \Phi_{\alpha}(B, E) dE = \int_0^{\infty} dE'' \int_0^{\infty} dE' \Sigma_o(E' \rightarrow E'') \Phi_{\alpha}(B, E') - \int_0^{\infty} \Sigma_s(E) \Phi_{\alpha}(B, E) dE \quad (22)$$

From the definition of $\Sigma_s(E)$ (Eq. 2), Eq. 22 can be written as

$$\begin{aligned} \int_0^{\infty} F(B, \alpha, E) \Phi_{\alpha}(B, E) dE &= \int_0^{\infty} dE' \Phi_{\alpha}(B, E') \int_0^{\infty} dE'' \Sigma_o(E' \rightarrow E'') - \int_0^{\infty} \Sigma_s(E) \Phi_{\alpha}(B, E) dE \\ \int_0^{\infty} F(B, \alpha, E) \Phi_{\alpha}(B, E) dE &= \int_0^{\infty} \Sigma_s(E') \Phi_{\alpha}(B, E') dE' - \int_0^{\infty} \Sigma_s(E) \Phi_{\alpha}(B, E) dE \\ \therefore \int_0^{\infty} F(B, \alpha, E) \Phi_{\alpha}(B, E) dE &= 0 \end{aligned}$$

Constraint 2. The energy transfer cross section is assumed to obey the condition of detailed balance which is described by

$$S M(E) = 0 \quad (23)$$

where $M(E)$ is the equilibrium Maxwellian neutron energy distribution at the moderator temperature T .

The principle of detailed balancing states that the transition probability per unit time for a reaction going one way in time multiplied by the density of states is equal to the transition probability for the same reaction but with the sense of time reversed multiplied by the density of states.

The condition of detailed balance for the energy transfer cross section used above can be written as

$$\sum_0 (E' \rightarrow E) M(E') = \sum_0 (E \rightarrow E') M(E). \quad (24)$$

Substituting Eq. 24 into the definition of $S \phi_\alpha(B, E)$ with $\phi_\alpha(B, E)$ given by $M(E)$ gives

$$S M(E) = \int_0^\infty \sum_0 (E' \rightarrow E) M(E') dE' - \sum_s(E) M(E)$$

$$S M(E) = \int_0^\infty \sum_0 (E \rightarrow E') M(E) dE' - \sum_s(E) M(E)$$

By Eq. 2

$$S M(E) = \sum_s(E) M(E) - \sum_s(E) M(E)$$

or

$$S M(E) = 0$$

In order to solve Eq. 18 for α and $\phi_\alpha(B, E)$, the quantities $F(B, \alpha, E)$, α , and $\phi_\alpha(B, E)$ are expanded in powers of B .

$$\alpha = \alpha_0 - \sum_{j=1}^{\infty} \alpha_{2j} (iB)^{2j} \quad (25)$$

$$F(B, \alpha, E) = \sum_{j=0}^{\infty} F_{2j}(\alpha, E) (iB)^{2j} \quad (26)$$

$$\phi_{\alpha}(B, E) = \sum_{j=0}^{\infty} \phi_{2j}(E) (iB)^{2j} \quad (27)$$

Eq. 18 and the conservation condition, Eq. 21, must be satisfied to each order in B^2 . Attention is restricted to the lowest eigenvalue of Eq. 18. This solution represents the decay of a fully thermalized neutron flux. The expanded form of Eq. 25 is

$$\alpha = \alpha_0 + D_0 B^2 - CB^4 + FB^6 + \dots \quad (28)$$

The decay constants measured in a pulsed experiment are fitted to Eq. 23 by the method of least squares.

Rewriting Eq. 18

$$F(B, \alpha, E) \phi_{\alpha}(B, E) = S \phi_{\alpha}(B, E) \quad (18)$$

and substituting into it Eq. 26 and Eq. 27, one obtains

$$\left[\sum_{\ell=0}^{\infty} F_{2\ell}(\alpha, E) (iB)^{2\ell} \right] \left[\sum_{m=0}^{\infty} \phi_{2m}(E) (iB)^{2m} \right] = \int_0^{\infty} \sum_0(E' \rightarrow E) \sum_{n=0}^{\infty} \phi_{2n}(E') (iB)^{2n} dE' - \sum_S(E) \sum_{n=0}^{\infty} \phi_{2n}(E) (iB)^{2n} \quad (29)$$

The convolution of two infinite series can be written as

$$\sum_{l=0}^{\infty} a_l \sum_{m=0}^{\infty} b_m = \sum_{n=0}^{\infty} \left\{ \sum_{j=0}^n a_j b_{(n-j)} \right\}. \quad (30)$$

Using Eq. 30, Eq. 29 can be written as

$$\begin{aligned} \sum_{n=0}^{\infty} \left\{ \sum_{j=0}^n F_{2j}(d, E) \phi_{2(n-j)}(E) \right\} (iB)^{2n} = \\ \sum_{n=0}^{\infty} (iB)^{2n} \left\{ \int_0^{\infty} dE' \Sigma_0(E' \rightarrow E) \phi_{2n}(E') - \Sigma_s(E) \phi_{2n}(E) \right\}. \end{aligned}$$

Collecting like terms

$$\sum_{n=0}^{\infty} (iB)^{2n} \left\{ \sum_{j=0}^n F_{2j}(d, E) \phi_{2(n-j)}(E) - S \phi_{2n}(E) \right\} = 0 \quad (31)$$

where

$$S \phi_{2n}(E) = \int_0^{\infty} dE' \Sigma_0(E' \rightarrow E) \phi_{2n}(E') - \Sigma_s(E) \phi_{2n}(E)$$

From Eq. 31 one obtains the set of integral equations

$$\sum_{j=0}^n F_{2j}(d, E) \phi_{2(n-j)}(E) = S \phi_{2n}(E) \quad (32)$$

The expansion of α is carried out simultaneously with the expansion of $F(B, d, E)$ to the same order.

The expansion of Eq. 19 can be carried out by writing the inverse tangent as an infinite series.

$$F(B, d, E) = \frac{B}{\tan^{-1} \frac{B}{\Sigma_s(E) + \Sigma_a(E) - \frac{d}{v}}} - \Sigma_s(E) \quad (19)$$

Using the expansion for $\tan^{-1} z$

$$\tan^{-1} z = z - \frac{z^3}{3} + \frac{z^5}{5} - \frac{z^7}{7} + \dots$$

$$F(B, d, E) = -\Sigma_s(E) + \frac{B}{\frac{B}{x} - \frac{B^3}{3x^3} + \frac{B^5}{5x^5} - \frac{B^7}{7x^7} + \dots}$$

where $x = \Sigma_s(E) + \Sigma_a(E) - \frac{d}{v}$

$$F(B, d, E) = -\Sigma_s(E) + \Sigma_s(E) + \Sigma_a(E) - \frac{d}{v} + \frac{B^2}{3[\Sigma_s(E) + \Sigma_a(E) - \frac{d}{v}]^2} - \frac{4B^4}{45[\Sigma_s(E) + \Sigma_a(E) - \frac{d}{v}]^3} + O(B^6)$$

$$F(B, d, E) = \Sigma_a(E) - \frac{d}{v} + \frac{B^2}{3[\Sigma_s(E) + \Sigma_a(E) - \frac{d}{v}]^2} - \frac{4B^4}{45[\Sigma_s(E) + \Sigma_a(E) - \frac{d}{v}]^3} + O(B^6) \tag{33}$$

Expanding $F(B, d, E)$ by Eq. 26

$$F(B, d, E) = F_0(d, E) - F_2(d, E)B^2 + F_4(d, E)B^4 + \dots O(B^6) \tag{34}$$

Recalling that d must be expanded also, Eq. 33 becomes

$$F(B, d, E) = \Sigma_a(E) - \frac{d_0}{v} - \frac{D_0 B^2}{v} + \frac{C B^4}{v} + \frac{B^2}{3\left\{\Sigma_s(E) + \Sigma_a(E) - \frac{d_0}{v} - \left(\frac{D_0 B^2 - C B^4}{v}\right)\right\}^2} - \frac{4B^4}{45\left\{\Sigma_s(E) + \Sigma_a(E) - \frac{d_0}{v} - \left[\frac{D_0 B^2 - C B^4}{v}\right]\right\}^3} + O(B^6)$$

$$F(B, d, E) = \Sigma_a(E) - \frac{d_0}{V} - \frac{D_0 B^2}{V} + \frac{C B^4}{V} + \frac{B^2}{3 \{ \Sigma_s(E) + \Sigma_a(E) - \frac{d_0}{V} \}} \left[\frac{1}{1 - \frac{D_0 B^2 - C B^4}{V \{ \Sigma_s(E) + \Sigma_a(E) - \frac{d_0}{V} \}}} \right] - \frac{4 B^4}{45 \{ \Sigma_s(E) + \Sigma_a(E) - \frac{d_0}{V} \}^3} \left[\frac{1}{1 - \frac{D_0 B^2 - C B^4}{V \{ \Sigma_s(E) + \Sigma_a(E) - \frac{d_0}{V} \}}} \right]^3 + O(B^6)$$

$$F(B, d, E) = \Sigma_a(E) - \frac{d_0}{V} - \frac{D_0 B^2}{V} + \frac{C B^4}{V} + \frac{B^2}{3 \{ \Sigma_s(E) + \Sigma_a(E) - \frac{d_0}{V} \}} \left[1 + \frac{D_0 B^2 - C B^4}{V \{ \Sigma_s(E) + \Sigma_a(E) - \frac{d_0}{V} \}} + \dots \right] - \frac{4 B^4}{45 \{ \Sigma_s(E) + \Sigma_a(E) - \frac{d_0}{V} \}^3} \left[1 + \frac{3(D_0 B^2 - C B^4)}{V \{ \Sigma_s(E) + \Sigma_a(E) - \frac{d_0}{V} \}} + \dots \right] + O(B^6)$$

$$F(B, d, E) = \Sigma_a(E) - \frac{d_0}{V} - B^2 \left[\frac{D_0}{V} - \frac{1}{3 \{ \Sigma_s(E) + \Sigma_a(E) - \frac{d_0}{V} \}} \right] + B^4 \left[\frac{C}{V} + \frac{D_0}{3V \{ \Sigma_s(E) + \Sigma_a(E) - \frac{d_0}{V} \}^2} - \frac{4}{45 \{ \Sigma_s(E) + \Sigma_a(E) - \frac{d_0}{V} \}^3} \right] + \dots \quad (35)$$

Equating coefficients in Eq. 34 and Eq. 35

$$F_0(d, E) = \Sigma_a(E) - \frac{d_0}{V} \quad (36)$$

$$F_2(d, E) = \frac{D_0}{V} - \frac{1}{3 \{ \Sigma_s(E) + \Sigma_a(E) - \frac{d_0}{V} \}} \quad (37)$$

$$F_4(d, E) = \frac{C}{V} + \frac{D_0}{3V \{ \Sigma_s(E) + \Sigma_a(E) - \frac{d_0}{V} \}^2} - \frac{4}{45 \{ \Sigma_s(E) + \Sigma_a(E) - \frac{d_0}{V} \}^3} \quad (38)$$

To lowest order then Eq. 32 becomes

$$\left[\Sigma_a(E) - \frac{d_0}{V} \right] \phi_0(E) = S \phi_0(E) \quad (38)$$

The lowest eigenvalue of Eq. 37 corresponds to the decay of a fully thermalized pulse in an infinite medium with no spatial variation.

For a $1/v$ absorber,

$$\phi_0(E) = M(E)$$

a Maxwellian distribution. By Eq. 23, the right side of Eq. 38 vanishes which implies

$$\alpha_0 = v \sum_a(E) \quad (39)$$

For $n = 1$ Eq. 32 becomes

$$F_0(d, E) \phi_2(E) + F_2(d, E) \phi_0(E) = S \phi_2(E) \quad (40)$$

for a $1/v$ absorber $F_0(d, E) \phi_2(E) = 0$ and Eq. 40 becomes

$$F_2(d, E) M(E) = S \phi_2(E) \quad (41)$$

Integrating Eq. 41 with respect to energy and applying the neutron conservation condition

$$\int_0^{\infty} F_2(d, E) M(E) dE = 0 = \int_0^{\infty} S \phi_2(E) dE$$

$$\int_0^{\infty} \left[\frac{D_0}{v} - \frac{1}{3 \Sigma_s(E)} \right] M(E) dE = 0 \quad (42)$$

Solving Eq. 42 for D_0

$$\int_0^{\infty} \frac{D_0}{v} M(E) dE = \int_0^{\infty} \frac{1}{3 \Sigma_s(E)} M(E) dE$$

then $D_0 = \frac{\int_0^{\infty} \frac{1}{3 \Sigma_s(E)} M(E) dE}{\int_0^{\infty} \frac{1}{v} M(E) dE} \quad (43)$

Eq. 41 becomes

$$\left[\frac{D_0}{V} - \frac{1}{3 \Sigma_s(E)} \right] M(E) = S \phi_2(E) \quad (44)$$

Eq. 44 for $\phi_2(E)$ represents the shift of the spectrum to lower energies due to the increase in leakage rate with neutron velocity which is called diffusion cooling. The diffusion cooling is the dominant contribution to the decay constant to order B^4 .

For $n = 2$, Eq. 32 becomes

$$F_0(\alpha, E) \phi_4(E) + F_2(\alpha, E) \phi_2(E) + F_4(\alpha, E) \phi_0(E) = S \phi_4(E) \quad (45)$$

Integrating Eq. 45 over energy and applying the neutron conservation condition

$$\int_0^\infty [F_0(\alpha, E) \phi_4(E) + F_2(\alpha, E) \phi_2(E) + F_4(\alpha, E) \phi_0(E)] dE = \int_0^\infty S \phi_4(E) dE$$

which becomes

$$\int_0^\infty [F_2(\alpha, E) \phi_2(E) + F_4(\alpha, E) \phi_0(E)] dE = 0$$

For a $1/v$ absorber, $F_0(\alpha, E) \phi_4(E) = 0$

$$\therefore \int_0^\infty [F_2(\alpha, E) \phi_2(E) + F_4(\alpha, E) \phi_0(E)] dE = 0 \quad (46)$$

Substituting into Eq. 46 the values of $F_2(\alpha, E)$ and $F_4(\alpha, E)$ from Eqs. 37 and 38 respectively,

$$\int_0^\infty \frac{d}{V} M(E) dE + \int_0^\infty \frac{1}{3 \Sigma_s^2(E)} \left[\frac{D_0}{V} - \frac{4}{15 \Sigma_s(E)} \right] M(E) dE + \int_0^\infty \left[\frac{D_0}{V} - \frac{1}{3 \Sigma_s(E)} \right] \phi_2(E) dE = 0$$

Solving for C

$$C = \frac{\int_0^{\infty} \left[\frac{1}{3 \Sigma_s(E)} - \frac{D_0}{V} \right] \Phi_2(E) dE}{\int_0^{\infty} \frac{1}{V} M(E) dE} + \frac{\int_0^{\infty} \frac{1}{3 \Sigma_s^2(E)} \left[\frac{D_0}{V} - \frac{4}{15 \Sigma_s(E)} \right] M(E) dE}{\int_0^{\infty} \frac{1}{V} M(E) dE} \quad (47)$$

The diffusion cooling coefficient C is made up of two terms

$$C = C_D + C_T \quad (48)$$

where

$$C_D = \frac{\int_0^{\infty} \left[\frac{1}{3 \Sigma_s(E)} - \frac{D_0}{V} \right] \Phi_2(E) dE}{\int_0^{\infty} \frac{1}{V} M(E) dE} \quad (49)$$

C_D is related to the diffusion cooling of the spectrum in Eq. 44

and

$$C_T = \frac{\int_0^{\infty} \frac{1}{3 \Sigma_s^2(E)} \left[\frac{4}{15 \Sigma_s(E)} - \frac{D_0}{V} \right] M(E) dE}{\int_0^{\infty} \frac{1}{V} M(E) dE} \quad (50)$$

C_T represent the contribution to order B^4 due to deviations from diffusion theory and is independent of any deviations of the spectrum from a Maxwellian distribution.

In water for which the $1/v$ case applies approximately

$$C_T \simeq 1/5 C_D \quad (51)$$

By expanding Eq. 5 into spherical harmonics, the above results may be extended to the anisotropic scattering case. The coefficients of Eq. 28 are then given by Eqs. 39, 43, and 47 if $\sum_g(E)$ is replaced by $\sum \text{tr}(E)$.

ABSTRACT

The neutron diffusion parameters of water and ice were measured by the pulsed source method at two temperatures; 1.0°C. and -19°C.

Neutron pulses were obtained at one millisecond intervals by modulating the beam in a Cockcroft-Walton type accelerator. The ${}^1_1\text{H}^3(d,n){}^4_2\text{He}$ reaction was used to generate neutrons.

The samples were contained in cylindrical aluminum cans covered with cadmium. The experiment was conducted inside a large paraffin block which served as a neutron shield and thermal insulator. The temperature of the samples was maintained constant to within $\pm 1^\circ\text{C}$.

Neutrons leaving one surface of the sample were counted in a BF_3 proportional counter. The time distribution of these neutrons was recorded by an eighteen channel time analyser. The width of each channel was 20 microseconds. The opening of the first channel was delayed 100 microseconds with respect to the start of the neutron burst to minimize harmonics in the neutron decay.

A geometric buckling was calculated for each sized sample from

$$B^2 = \left[\frac{2.405}{R + \epsilon} \right]^2 + \left[\frac{\pi}{H + 2\epsilon} \right]^2 \quad (1)$$

where B^2 = geometric buckling

2.405 = first zero of J_0 Bessel Functions

R = radius of cylinder

H = height of cylinder

ϵ = extrapolation distance

The extrapolation distance ϵ was calculated from

$$\epsilon = 0.71 \lambda_{tr} \quad (2)$$

where λ_{tr} = mean free path of neutrons in water

The extrapolation distance was assumed to vary as $T^{1/2}$ where T is the temperature in degrees Kelvin.

The measured decay constants, α , were fitted by the method of least squares to a polynomial in B^2 of the form

$$\alpha = (\sum_a v) + D_0 B^2 - C B^4 \quad (3)$$

where

\sum_a = the macroscopic absorption cross section

v = the neutron velocity

D_0 = diffusion coefficient

C = diffusion cooling coefficient

The resultant values of $(\sum_a v)$ and D_0 for each temperature are below. The data did not permit a determination of C .

1.0°C. $(\sum_a v) = 4595 \pm 365 \text{ sec}^{-1}$, $D_0 = 29600 \pm 840 \text{ cm}^2/\text{sec}$

-19°C. $(\sum_a v) = 4355 \pm 263 \text{ sec}^{-1}$, $D_0 = 27050 \pm 630 \text{ cm}^2/\text{sec}$

